J. Am. Soc. Mass Spectrom. (2019) 30:2358–2368
DOI: 10.1007/s13361-019-02297-1

RESEARCH ARTICLE

Self-Supplied Liquid Injection Field Desorption/Ionization Ion Source for an Orthogonal Time-of-Flight Instrument

Mathias H. Linden,[1] H. Bernhard Linden,[1] Norbert Nieth,[2] Jürgen H. Gross[2]

[1]Linden CMS, Auf dem Berge 25, 28844, Weyhe, Germany
[2]Institute of Organic Chemistry, Heidelberg University, Im Neuenheimer Feld 270, 69120, Heidelberg, Germany

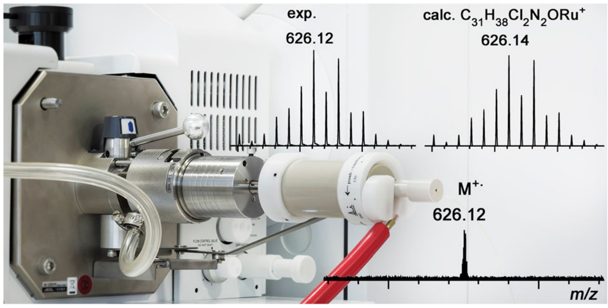

Abstract. A new implementation of a dedicated ion source for field ionization (FI), field desorption (FD), and liquid injection field desorption/ionization (LIFDI) for the JEOL AccuTOF GC series of orthogonal-acceleration time-of-flight instruments is presented. In contrast to existing implementations, this third-party LIFDI probe and source combination does not require the exchange of the entire ion source comprising ion source block and lens stack to switch from electron ionization (EI) to LIFDI. Rather, the methods may be swapped conveniently by only exchanging the ion source block for a mechanical probe guide and inserting the LIFDI probe in place of the standard direct insertion probe (DIP) via the vacuum lock. Further, this LIFDI setup does not require any changes of the electronics or software of the AccuTOF mass spectrometer because it is self-supplied in terms of power supply, observation optics, and computer control. The setup offers advanced FI/FD/LIFDI control features such as emission-controlled emitter heating current and emitter flash baking during elongated runs as required for gas chromatography-FI-mass spectrometry (MS). The LIFDI source and probe and its operation are reported in detail. FI spectra of the volatile analytes toluene, heptane, and pentafluoroiodobenzene are presented. LIFDI operation is demonstrated for the analysis of the saturated hydrocarbon dotriacontane and the low-mass hydrocarbon polymers polystyrene 484 and polystyrene 1050. Further, the air-sensitive 2nd-generation Hoveyda–Grubbs catalyst is analyzed by LIFDI-MS. For comparison with long-established LIFDI instrumentation, some of the spectra obtained with the new setup are also compared with those from a double-focusing magnetic sector instrument.

Keywords: Field ionization (FI), Field desorption (FD), Liquid injection field desorption ionization (LIFDI), Orthogonal time-of-flight analyzer, Magnetic sector analyzer, Alkanes, Polystyrene, Hoveyda–Grubbs II catalyst

Received: 24 May 2019/Revised: 17 July 2019/Accepted: 17 July 2019/Published Online: 2 August 2019

Introduction

Field ionization (FI), field desorption (FD), and liquid injection field desorption/ionization (LIFDI) form a family of ionization techniques that rely on the ability of strong electrostatic fields in the order of 10^8 V cm^{-1} (1 V $Å^{-1}$; 1 $Å = 10^{-10}$ m) to effect positive ionization of neutrals. The electric field is established by setting a sharp pin or edge (field anode) to positive high voltage (ca. 10 kV DC) with respect to a symmetrically aligned slotted counter electrode at about 2-mm distance. The field anode is normally termed field emitter as ions originate from there.

The phenomenon of field ionization was discovered in the mid-1950s [1, 2] and subsequently exploited for mass spectrometry by constructing FI ion sources [2–5]. First, FI was applied to analyze volatile liquids [6, 7] and later solids introduced by evaporation from a sample vial next to the ionizing

---

Electronic supplementary material The online version of this article (https://doi.org/10.1007/s13361-019-02297-1) contains supplementary material, which is available to authorized users.

Correspondence to: Jürgen Gross; *e-mail:* juergen.gross@oci.uni–heidelberg.de

electrode [8]. Thus, the term field ionization became used to describe the ionization mechanism and this particular experimental setup alike.

In contrast to FI, where samples need to be evaporated prior to undergoing gas phase ionization in close proximity to the emitter surface, FD combines ionization and subsequent desorption of the incipient analyte ions from the surface of the field emitter in a common process [9, 10].

Initially, sharp edges and bare thin wires were employed as field emitters. Today, activated field emitters bearing dendritic microneedles on the surface of a thin central wire are in use. Activation of 10–13-μm tungsten wires is normally performed by pyrolysis of benzonitrile or indene and subsequent precipitation of carbon onto the wire surface to grow fine needles in the presence of an electric field [11–14].

During FD operation, the emitter is resistively heated to effect surface mobility of the analyte and to assist desorption of analyte ions from its surface. Heating can be performed either at a constant rate (1–60 mA min^{-1}) or under emission control [15, 16]. The latter mode limits the emitter heating current (EHC) as soon as the ion emission current is approaching a preset limit. This prevents spark discharges between emitter wire and counter electrode that usually are fatal to the emitter. Most analytes desorb at EHCs in the 10–50-mA range, while EHCs of 90–120 mA are used to bake off residual sample before starting the next run.

Both FI and FD provide very soft positive ionization either by withdrawal of an electron from the analyte molecule by virtue of the strong electric field or by simply desorbing cationic analyte species into the gas phase [17–19]. FI and FD spectra often exhibit only a negligible degree of fragmentation. Thus, the methods are well suited for non-polar to polar and even ionic analytes [20–35]. As a rule of thumb, FD allows dealing with analytes of up to about 2500 u molecular mass.

LIFDI, essentially an improved sample introduction technique for FI and FD, enables sample introduction under inert conditions, i.e., an analyte solution stored under inert gas can be transferred onto the emitter inside the ion source vacuum without getting into contact with moisture and/or air. In addition, this technique allows for higher sample throughput due to shorter acquisition times and less tedious ion source tuning [36].

This is achieved by loading the emitter in vacuum by introducing the analyte solution through a fused silica transfer capillary (50–75 μm i.d.) from the laboratory into the ion source. The solvent evaporates within seconds, and thus, the emitter is getting ready for operation. Positioning of this transfer capillary and controlling the sample transfer require the observation of the capillary via a microscopic camera. The ability of LIFDI for the analysis of samples highly sensitive to moisture and oxygen has a proven record [36–49]. Moreover, LIFDI exhibits some potential for continuous-flow and even automated applications [50, 51].

According to the instrumentation available in the 1970s and 1980s, FI and FD matured in combination with magnetic sector mass spectrometers. Today, magnetic sector instruments have mostly been replaced by various other types of mass analyzers such as time-of-flight (TOF), quadrupole-time-of-flight (Q-TOF), Orbitrap, and Fourier transform-ion cyclotron resonance (FT-ICR) analyzers that either are much more compact and less power consuming or offer superior mass resolving power and mass accuracy. To preserve the unique capabilities of FI, FD, and LIFDI, these methods have to comply with the mass analyzers running in modern MS laboratories [46–51].

This work introduces a new dedicated LIFDI setup developed for the JEOL AccuTOF GC series of instruments, which belong to the orthogonal-acceleration time-of-flight mass spectrometers. They are designed for use with electron ionization (EI) and chemical ionization (CI) sources in combination with sample admission via a gas chromatograph (GC), a direct insertion probe (DIP), or a reservoir inlet. These instruments offer high resolution (10,000 FWHM), can provide accurate mass, and can cover the range *m/z* 4–6400 (AccuTOF GCx at 2-GHz sampling rate).

For the JEOL AccuTOF GC series, both a dedicated FI/FD source and a FI/FD/EI combination source are commercially available from the instrument manufacturer and also permit the adaptation of a LIFDI probe. The novelty of our new LIFDI probe and source combination is that it—unlike the instrument manufacturer's original implementation—does not require the exchange of the entire ion source comprising ion source block and focusing lens stack to switch from either EI or CI to FI/FD/LIFDI mode. Additionally, the GC interface remains untouched when switching ionization methods. Rather, the methods may be swapped in a much more convenient manner within a few minutes by simply exchanging the ion source block for a mechanical probe guide and inserting the LIFDI probe in place of the standard direct insertion probe (DIP) via the vacuum lock. Moreover, this design of a LIFDI source does not require any changes of AccuTOF mass spectrometer's electronics or software as it is self-supplied in terms of power supply, observation optics, and computer control. The setup also enables advanced FI/FD/LIFDI control features such as emission-controlled emitter heating current and emitter flash baking during elongated runs as required for gas chromatography-FI experiments [52–54].

Here, we describe this new LIFDI source and probe, report on its operation in FI and LIFDI modes, and compare some of the results obtained with this new setup with those from a JEOL JMS-700 double-focusing magnetic sector instrument.

Experimental

Analytes Toluene, heptane, and pentafluoroiodobenzene (PFIB) were obtained from Sigma-Aldrich (Steinheim, Germany) and used as a liquid sample for admission of sample vapor via the transfer capillary in FI mode. For LIFDI mode, the saturated hydrocarbon dotriacontane (Fluka, Buchs, Switzerland), the low-mass polymers polystyrene 484 and 1050 (Federal Institute for Materials Research and Testing, BAM, Berlin, Germany), Balzers P3 rough pump oil (Oerlikon Balzers Coating Germany GmbH, Bingen, Germany), and the air-sensitive

Hoveyda–Grubbs II catalyst ((1,3-dimesitylimidazolidin-2-ylidene)(2-isopropoxybenzylidene)ruthenium(VI) chloride) (Sigma-Aldrich, Steinheim, Germany) were dissolved in toluene and used at concentrations of 0.2–0.6 mg mL^{-1} in solution. The ionic liquids *N*-butyl-3-methylpyridinium dicyanamide and 1-butyl-1-methylpyrrolidinium bis(trifluormethylsulfonyl)imide (Merck KGaA, Darmstadt, Germany) were used as solutions in methanol (Sigma-Aldrich, Steinheim, Germany) at 0.1 µL mL^{-1}. The analytes are compiled in Table 1.

AccuTOF GCx Instrument and LIFDI Source The JEOL AccuTOF GCx orthogonal-acceleration time-of-flight mass spectrometer (JEOL, Tokyo, Japan) was used. To switch from EI to LIFDI operation, the ion source housing was vented and the vacuum lock for the direct insertion probe (DIP) was unmounted. The EI ion source block was removed and replaced by a mechanical guide for the LIFDI probe. All other parts of the ion source such as lens stack for ion focusing, interfaces to reservoir inlet, and gas chromatograph remained untouched (Figure 1). Next, the ion source housing was evacuated for at least 30 min and the source was heated to 50 °C while the reservoir and the GC interface were set to 90 °C. The Supplementary Material provides images showing the setup, the LIFDI probe, screenshots of emitter observation, and ion source components (Figures S1–S7).

All components used for LIFDI operation were manufactured by Linden CMS (Weyhe, Germany). Emitter high voltage and emitter heating current were controlled using the Linden LIFDI-700 electronics and LIFDI-700 control software. An activated tungsten wire emitter (type LIFDI 413) based on a 13-µm wire was fitted to the tip of the probe. The counter electrode was then attached to the probe tip. Having the counter electrode on the probe allows cleaning of this part without venting the ion source, e.g., each time the field emitter is replaced. Next, the LIFDI probe was inserted via the vacuum lock following the procedure as established in DIP operation and pushed into a position about 30 mm off its final position for LIFDI operation. A USB microscopic camera (25-mm focal length, ca. × 25 magnification) was placed on top of the ion source housing's cover glass to allow for visual inspection of the emitter and for the precise adjustment of the sample transfer capillary as to enable wetting of the activated emitter by sample solution. Testing of correct emitter wetting and purging of the capillary between analytical runs were performed using pure solvents.

Instrument tuning was performed on the molecular ion of either toluene, *m/z* 92, or pentafluoroidobenzene, *m/z* 294, admitted as vapor via the sample transfer capillary. This fused silica capillary had an inner diameter of 75 µm and a length of 75 cm. The onset of signals started at a counter electrode potential of − 6 kV. The full potential of − 10 kV was used for tuning and for all measurements. To accelerate the ions generated at the emitter into the ion focusing lens stack of the JEOL instrument, the emitter was set to a potential of + 42 V. All ion source voltages were optimized using the instrument's built-in tuning routine. With a fresh emitter and the detector voltage set to 2800 V, the toluene molecular ion was normally observed at a signal intensity of 80–150 k counts at 6500 resolving power (FWHM).

External Mass Calibration External mass calibration was performed in LIFDI mode by measuring a mixture of PS 484 and PS 1050 in toluene using a mass reference list based on the *m/z* values provided in Table 1 [55]. When the screw cap septum vial with calibrant solution was not removed from the capillary during data acquisition, the toluene molecular ion was present in addition to the PS molecular ion series, thereby providing a low-mass calibration point at *m/z* 92. The upper limit covered by this mixture was *m/z* 2035. Generally, the *m/z* values based on this external calibration were within 0.01–0.02 u of the calculated value. Hence, experimental *m/z* values are reported here with two digits after the decimal point.

Table 1. Compounds Analyzed by FI or LIFDI in This Study

Compound name	Composition	Calc. *m/z* of $M^{+\bullet}$ ion(s) or cation	Measured by*
Toluene	C_7H_8	92.0620	FI @ TOF
Heptane	C_7H_{16}	100.1246	FI @ TOF & BE
Pentafluoroiodobenzene	C_6F_5I	293.8959	FI @ TOF
Dotriacontane	$C_{32}H_{66}$	450.5159	LIFDI @ TOF & BE
Polystyrene 484	$C_4H_{10}(C_8H_8)_n$	370.2655, 474.3281, 578.3907, 682.4533, 786.5159, 890.5785	LIFDI @ TOF
Polystyrene 1050	$C_4H_{10}(C_8H_8)_n$	474.3281, 578.3907, 682.4533, 786.5159, 890.5785, 994.6411, 1098.7037, 1202.7663, 1306.8289, 1410.8915, 1514.9541, 1619.0167, 1723.0793, 1827.1419, 1931.2045, 2035.2671	LIFDI @ TOF
Hoveyda–Grubbs II catalyst	$C_{31}H_{38}Cl_2N_2O^{102}Ru$	626.1402 (most abundant)	LIFDI @ TOF & BE
N-Butyl-3-methylpyridinium dicyanamide	$[C_{10}H_{16}N]^+ [C_2N_3]^-$	150.1277	LIFDI @ TOF
1-Butyl-1-methylpyrrolidinium bis(trifluormethylsulfonyl)-imide	$[C_9H_{20}N]^+ [C_2F_6NO_4S_2]^-$	142.1590	LIFDI @ TOF
Balzers P3 rough pump oil	Hydrocarbons	–	LIFDI @ TOF

*TOF denotes JEOL AccuTOF GCx; BE denotes JEOL JMS-700 magnetic sector instrument

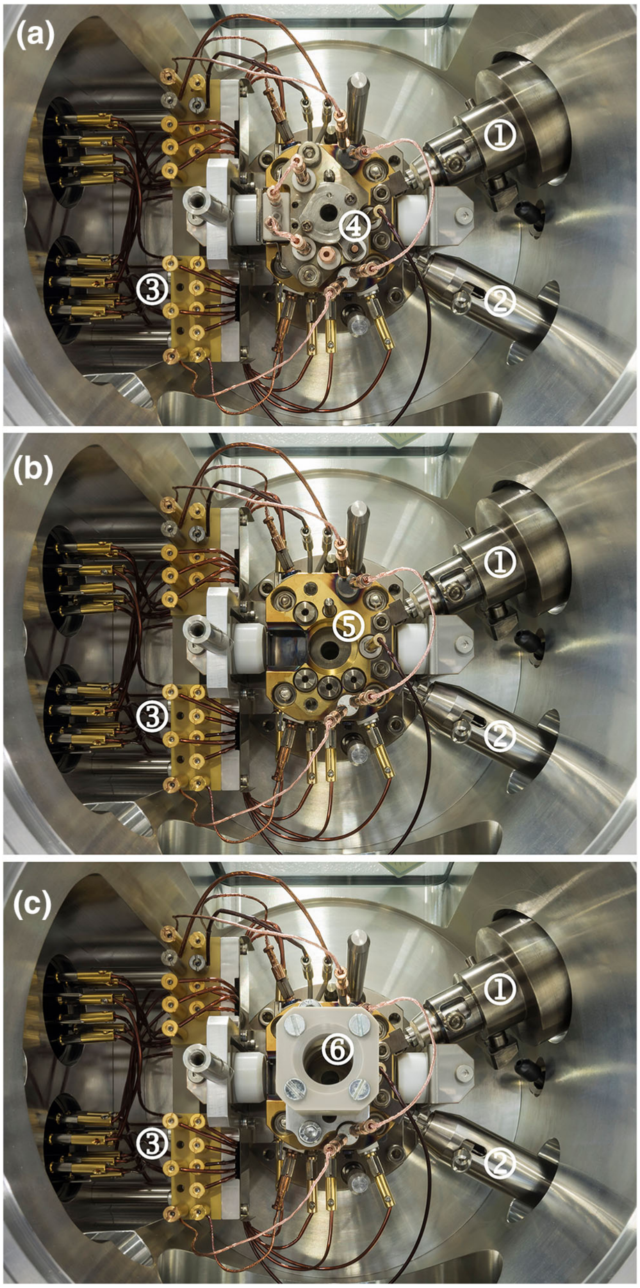

Figure 1. Sequence of swapping the ion sources from EI/CI operation to LIFDI operation. (**a**) View into the ion source housing of the JEOL AccuTOF with the EI source block for operating the direct insertion probe installed. (**b**) After unscrewing two Allen screws the EI source block has been withdrawn from the ion focusing optics stack. Both GC interface and reservoir inlet connector remain untouched. (**c**) The LIFDI probe guide has been mounted in place of the EI source. The components are as follows: (1) GC interface, (2) reservoir inlet, (3) electric supplies, (4) EI source block, (5) source after removal of EI source block, (6) probe guide for LIFDI in place. Essentially, only (4) is replaced by (6) while all other parts remain untouched

Once established, the tuning parameters and mass calibration were saved as a JEOL AccuTOF method file that was loaded and fine-tuned each time after mounting the LIFDI source. Typical settings are compiled in Table 2. The positioning of the emitter, and consequently the source parameters, was highly reproducible calling for only minor adjustments after replacement of an emitter or reinstallation of the source.

Procedure of FI/FD/LIFDI Operation Due to the third-party character of this setup, the initialization of data acquisition and the control of the LIFDI hardware run independent of each other. The AccuTOF mass spectrometer is controlled using the JEOL's MS Axel software while the FI/FD/LIFDI hardware is controlled via the LIFDI-700 unit's software. In brief, the counter electrode potential is raised in1-kV steps to -10 kV. In FI mode, the emitter is operated at an EHC of 0 mA, while in FD/LIFDI mode the emitter heating is started at the beginning of data acquisition at a rate of 20–52 mA min^{-1}. Fast EHC ramping is preferred because it (a) shortens the time available for thermal decomposition of the analyte, (b) causes higher desorption/ionization rates leading to enhanced signal intensity, and (c) speeds up the overall analysis (the LIFDI-700 unit allows up to 60 mA min^{-1}). Due to emission-controlled EHC (maximum ion emission current of 1.0×10^{-5} A), the EHC ramp would be lowered if the analyte would undergo too rapid ionization. Thus, emitter rupture due to sudden desorption/ionization and subsequent spark discharge are avoided. Finally, the emitter is cleaned by baking it for 1–2 s at 100–120 mA. A detailed description of the procedure and a screenshot of the LIFDI-700 software are provided in the Supplementary Material (Figure S8).

AccuTOF GCx Data Acquisition in FI and LIFDI Mode Depending on the actual *m/z* range, the AccuTOF GCx instrument can acquire up to 1600 TOF spectra per second. However, the actual number of TOF spectra per second is not reported in the data. Essentially, the instrument is continuously acquiring TOF spectra for the period defined as accumulation time and then transfers the accumulated spectrum to the PC (in our case 0.995 s of accumulation and 0.005 s wait time, Table 2).

All FI spectra were obtained by averaging an acquisition period of 60 s. LIFDI spectra were obtained by averaging across the period of desorption/ionization of the respective analyte, typically 20 to 40 s. The exact period (as a fraction of minute) is stated in the top left corner of the spectral plots, e.g., in Figure 4b, MS: 0.8686–1.5353.

Magnetic Sector Instrument A JEOL JMS-700 (JEOL, Tokyo, Japan) double-focusing reversed-geometry magnetic sector instrument was equipped with a LIFDI probe (Linden CMS, Leeste, Germany) previously described in detail [34, 37]. In brief, the LIFDI setup consists of a probe, observation optics, and a window for emitter illumination at the side of the ion source housing. In this configuration, the LIFDI probe simply replaces the JEOL FI/FD probe. The instrument was set to scan the *m/z* 40–800 range in 12 s with the resolving power adjusted to $R_{10\%} = 1500$. An ion acceleration voltage of 7 kV was

Table 2. Typical Instrument Tuning Parameters for AccuTOF GCx in LIFDI Operation

Basic settings		**Advanced settings**	
Ion chamber	50 °C	Ion source	35 V
Reservoir	90 °C	Reflectron	1150 V
GC interface	90 °C	Push	777.8 V
Repeller	1.6 V	Pull	− 777.8 V
Lens 1	− 1000 V	Suppress	0.20 V
Lens 2	− 680 V	Flight tube	−7000 V
Lens 3	− 75 V		
Slit lens	− 25 V	**Acquisition**	
Deflector	− 50 V	Sampling interval	0.5 ns
Lens 2 balance	− 20 V	Recording interval	1.00 s
Deflector balance	− 2.2 V	Accumulation time	0.995 s
Push bias	− 0.15 V	Wait time	0.005 s
Detector	2800 V	*m/z*	50–2400
Vacuum			
Ion source	2.5–4.0 × 10^{-3} Pa		
Analyzer	2.0–5.0 × 10^{-5} Pa		

employed. For tuning, toluene was admitted to the ion source from the reservoir inlet and field ionized to yield the molecular ion peak at *m/z* 92. The unmodified manufacturer's FD/FI ion source was used and the emitter potential was 10.0 kV. Activated tungsten wire (13 μm) LIFDI emitters (Linden CMS, Leeste, Germany) were employed. During the experiments, the emitter heating current (EHC) was ramped from 2 to 40 mA at 8 mA min^{-1}. Repeated short baking at 90mA was used to clean the emitter after each measurement.

For FI spectra, a screw cap septum vial with the liquid was attached to the transfer capillary to continuously admit sample vapor from the headspace into the ion source. For LIFDI spectra, the atmospheric pressure entrance of the capillary was dipped into the sample solution for 3 s whereby sample solution was sucked onto the emitter inside the ion source. The transfer through the capillary took about 10 s; further 30–60 s was necessary to allow for evaporation of the solvent and for further pumping to recover the ion source vacuum. (The aged JMS-700 had the original 520 L s^{-1} turbomolecular pump at the ion source housing replaced by a 240 L s^{-1} pump.)

Results and Discussion

Field Ionization of Volatile Compounds Volatile analytes are measured in FI mode, i.e., gaseous analyte is admitted as to pass along the activated field emitter for ionization. In classical FI sources, the sample vapor is admitted to the ion source via a reservoir inlet, while in combination with the LIFDI probe the transfer capillary presents an alternative way of introducing the gaseous sample. In fact, attaching a screw cap septum vial with the volatile liquid to the laboratory end of this capillary presents the more convenient way of FI sample supply. This technique offers highly reproducible sample flow as its flow solely depends on the vapor pressure of the analyte and the physical dimensions of the transfer capillary as long as the same type of capillary is employed and the temperature of the sample vial (essentially temperature of the laboratory) remains constant. Furthermore, switching between samples is speeded up because the continuous air flow from the atmosphere into the ion source effectively flushes the capillary in 10–15 s without further ado, whereas the reservoir inlet takes time to pump out the preceding sample.

FI is thus convenient for the analysis of solvents and mixtures thereof, and more importantly for FI/FD/LIFDI applications, the FI mode provides a continuous signal for instrument tuning. The molecular ions of acetone, $[C_3H_6O]^{+\bullet}$, *m/z* 58, and toluene, $[C_7H_8]^{+\bullet}$, *m/z* 92, are commonly used for this purpose while pentafluoroidobenzene (PFIB), $[C_6F_5I]^{+\bullet}$, *m/z* 294, offers the advantage that tuning is not performed at the very low-mass end of the *m/z* range that may even not be accessible by some instruments [56].

The FI mass spectra of toluene, heptane, and PFIB as obtained by sample introduction from a screw cap septum vial via the transfer capillary are shown in Figure 2. Immediately before starting spectral acquisition, the emitter was baked for 2 s at 120 mA. Then, data was accumulated for 1 min. Toward the end of those 1-min acquisitions, the molecular ion intensity dropped to circa half of the initial intensity due to slow emitter deactivation. The final spectra were obtained by averaging across this range to obtain representative intensity values. Each compound was analyzed in triplicate to ensure that the intensities and noise levels were reproducible (Supplementary Figures S9–11).

The respective molecular ions were detected as peaks of 72 to 87 k counts intensity, which is about 10 times less than when acquiring EI spectra of volatile compounds by sample admission via the reservoir inlet. To judge this properly, one has to take into account that ion currents in FI intrinsically are about three orders of magnitude lower than those in EI [57]. This is also evident from JEOL's instrument specifications stating that in EI mode, 10^{-12} g of octafluoronaphthalene yields a signal-to-noise ratio (s/n) of 300 while their FI sources yield a s/n of 40 with 10^{-10} g of hexadecane. The just ten times lower number of counts in FI spectral intensity is due to our setting of the detector voltage at 2800 V versus 2160 V in EI. Thus, the detector roughly compensates two orders of magnitude by providing higher amplification. Measuring the signal-to-noise

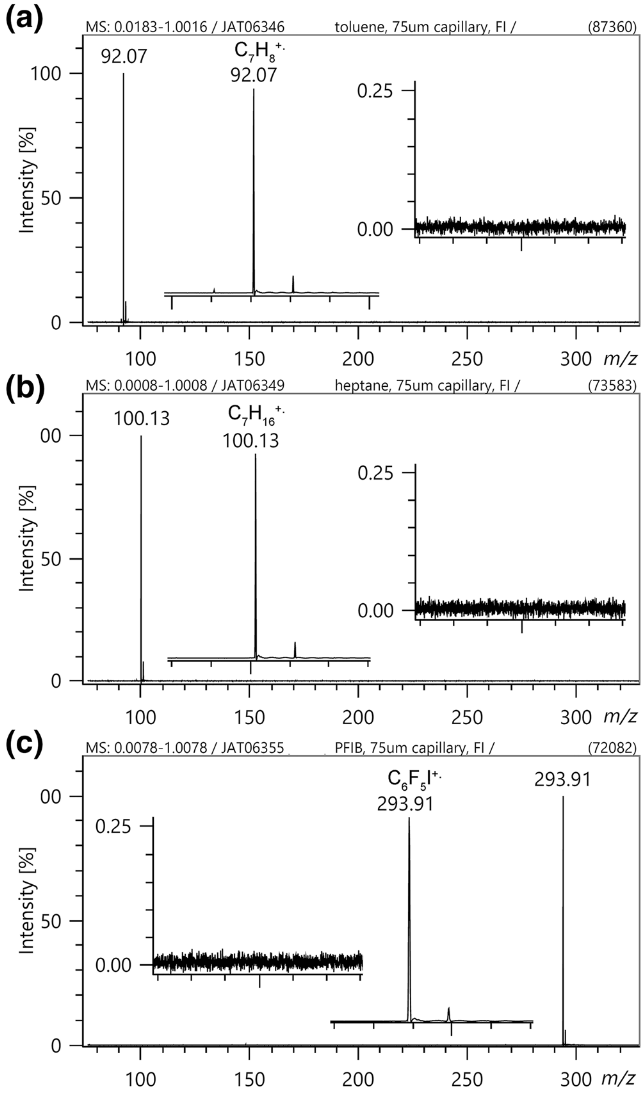

Figure 2. FI mass spectra of (**a**) toluene, *m/z* 92.07; (**b**) heptane, *m/z* 100.13; and (**c**) PFIB, *m/z* 293.91, as obtained by sample introduction from a screw cap septum vial via the transfer capillary. The spectra are averages of 1-min acquisitions. The insets show the respective molecular ions and the noise levels in expanded view. The numbers in parentheses at the upper right corner state the intensity in counts

ratio provides a more useful comparison of spectral quality. All FI spectra exhibited a noise level of around 0.03% relative intensity, i.e., s/n of about 3300. This is highly satisfactory when comparing it to the noise level of around 0.01% relative intensity, i.e., a s/n of about 10,000 in EI spectra.

The FI mass spectrum of toluene shows the monoisotopic molecular ion, $[C_7H_8]^{+\bullet}$, at *m/z* 92.07 (calc. *m/z* 92.0620) accompanied by the ^{13}C isotopic peak at *m/z* 93.07 of 8.9% relative intensity (calc. 7.7%). Analogously, the FI mass spectrum of heptane exhibits the monoisotopic molecular ion, $[C_7H_{16}]^{+\bullet}$, at *m/z* 100.13 (calc. *m/z* 100.1246) and the ^{13}C isotopic peak at *m/z* 101.14 of 8.1% relative intensity (calc. 7.7%), both *m/z* and intensities being in accordance with calculated values. The spectrum of PFIB shows the molecular ion, $[C_6F_5I]^{+\bullet}$, at *m/z* 293.91 (calc. *m/z* 293.8959), and the ^{13}C isotopic peak at *m/z* 294.91 and 6.5% relative intensity (calc. 6.6%). The slight overestimation of the ^{13}C isotopic peak in the case of toluene may be attributed to the formation of protonated toluene, $[C_7H_9]^+$, i.e., of about 1% of the molecules. Protonation in addition to molecular ion formation is a process known to occur in FI [58, 59].

LIFDI of Dotriacontane The aliphatic hydrocarbon dotriacontane, $C_{32}H_{66}$, is a solid at room temperature and needs to be applied in solution to the emitter. The compound was used as solution at 0.2 mg mL^{-1} in toluene and supplied to the emitter by dipping the transfer capillary for 2 s into this solution. After about 30 s, the emitter high voltage was set and data acquisition as well as emitter heating at 30 mA min^{-1} was started.

The LIFDI spectrum of dotriacontane (Figure 3) is dominated by the molecular ion peak at *m/z* 450.49 (calc. *m/z* 450.5159) accompanied by the ^{13}C peak (exp. 36.2%, calc. 35.2%). A closer look reveals some peaks at even *m/z* values, i.e., two below at *m/z* 422.46 (1.6%) and *m/z* 436.47 (1.2%) and one above at *m/z* 464.50 (0.5%) that can be assigned to impurities, i.e., to molecular ions of $C_{30}H_{62}$, $C_{31}H_{64}$, and $C_{33}H_{68}$, respectively. In addition, there are several minor peaks at odd *m/z* values, basically all at $\Delta(m/z) = 14$ ranging from *m/z* 281.31 to *m/z* 421.45, that can be attributed to eliminations of radicals from $C_2H_5^\bullet$ to $C_{12}H_{25}^\bullet$ by the molecular ion. The most intensive peak at *m/z* 393.42 (2.5%) of this fragment ion series corresponds to loss of a butyl radical. While the noise level is again very good at just 0.05% relative intensity (s/*n* = 2000), the spectrum is not perfectly free from fragment ion signals. The spectrum has also been acquired in triplicate to ensure that the intensities and noise levels were reproducible (Supplementary Figure S12).

LIFDI of Polystyrenes The ability of FD-MS to softly ionize non-functionalized molecules renders it well suited for the analysis of large hydrocarbons and low-mass hydrocarbon polymers such as polyethylenes and polystyrenes [27, 30–32, 55, 56, 60].

Two polystyrenes, PS 484 and PS 1050, were subjected to LIFDI-MS as 0.5 mg mL^{-1} solutions in toluene; the PS 1050 sample had previously been analyzed by LIFDI-FT-ICR-MS [56]. As expected, the spectra showed the molecular ions at $\Delta(m/z) = 104$ and revealed the molecular weight distributions of these samples (Figure 4). In case of PS 484, the series of molecular ions started with the 3mer, $[(C_8H_8)_3C_4H_{10}]^{+\bullet}$, *m/z* 370.26 (calc. *m/z* 370.2655), and continued up to the 9mer, $[(C_8H_8)_9C_4H_{10}]^{+\bullet}$, *m/z* 890.57 (calc. *m/z* 890.5785). The spectrum of the PS 1050 sample showed molecular ions from the 4mer, $[(C_8H_8)_4C_4H_{10}]^{+\bullet}$, *m/z* 474.33 (calc. *m/z* 474.3281), up to the 19mer, $[(C_8H_8)_{19}C_4H_{10}]^{+\bullet}$, *m/z* 2035.32 (calc. *m/z* 2035.2671). The latter also was the last to be included as reference for mass calibration. From the 11mer upward, the first ^{13}C isotopic ion peaks exceeded the intensity of the

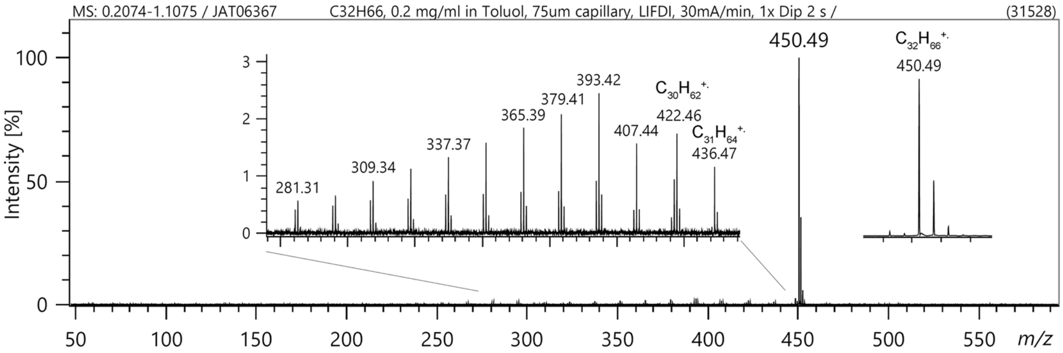

Figure 3. LIFDI mass spectrum of dotriacontane, $C_{32}H_{66}$, showing the $M^{+\bullet}$ ion at *m/z* 450.49. The spectrum is the average across the period of ion desorption. The insets show the molecular ion signal and the range of low-intensity fragment ions in expanded view. The number in parentheses at the upper right corner states the intensity in counts

monoisotopic species. These spectra also exhibited a noise level of around 0.03% relative intensity, i.e., a signal-to-noise ratio of about 3300, and were acquired in triplicate to ensure that the intensities and noise levels were reproducible (Supplementary Figures S13–S14).

LIFDI for the Analysis of Air- and Moisture-Sensitive Compounds As mentioned in the "Introduction," one of the strengths of LIFDI over conventional FD is the ability to transfer a sample to the field emitter under inert conditions [36–49]. This presents a marked difference to approaches based on some sort of off-line sampling, e.g., sample deposition onto the emitter in a glove box, as this cannot circumvent the need to finally take the emitter out of the inert environment, to put it onto the probe, and to subsequently mount the probe to the vacuum lock. Even doing that quickly takes tens of seconds and other techniques like working in an argon-filled plastic bag or under a transparent housing are simply not practical.

The range of solvents acceptable for LIFDI is not exclusively defined by the reactivity of the analyte but additionally by the need to evaporate reasonably quickly without freezing upon evaporation in vacuum. From a technical point, toluene, tetrahydrofuran, chloroform, dichloromethane, ethyl acetate, acetone, and methanol fulfill these criteria very well. Water and acetonitrile, on the other hand, freeze and therefore fail to wet the emitter while dimethylformamide and dimethyl sulfoxide take tens of minutes to evaporate. In unfortunate cases, analytes of very low solubility (< 0.05 mg mL^{-1}) or of extremely high reactivity may precipitate during cooling of the solvent upon evaporation or following decomposition, respectively. Such events can cause temporary clogging of the transfer capillary.

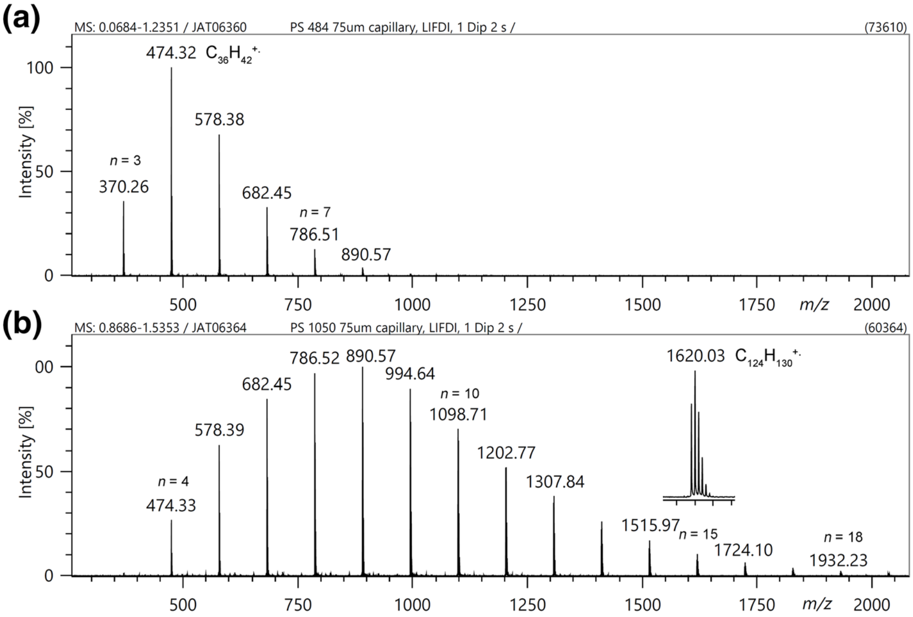

Figure 4. LIFDI mass spectra of (**a**) PS 484 and (**b**) PS 1050. The low-mass polymers are detected as molecular ions, in (**a**) ranging from the 3mer to 8mer and in (**b**) from the 4mer to the 19mer. Note that up to the 11mer the *m/z* labels refer to monoisotopic ions while thereafter the label refers to the first ^{13}C isotopic ion. The spectra are averages across the period of ion desorption. The inset in (**b**) shows the molecular ion signal of the 15mer, $C_{124}H_{130}^{+\bullet}$, in expanded view. The number in parentheses at the upper right corner states the intensity in counts

Also, residues from preceding runs need to be purged out of the capillary by repeated flushing with solvent followed by baking of the emitter to remove the contaminant.

As an example of an air- and moisture-sensitive compound, the Hoveyda–Grubbs II catalyst, $C_{31}H_{38}Cl_2N_2ORu$, has been examined. The catalyst was dissolved in toluene at 0.6 mg mL $^{-1}$ and transferred onto the emitter from a screw cap septum vial by dipping the transfer capillary into the solution. Keeping the entrance of the capillary in the screw cap septum vial caused a toluene molecular ion peak, *m/z* 92.08, to be present at all times during the run (Figure 5). The catalyst formed a molecular ion, $[C_{31}H_{38}Cl_2N_2ORu]^{+\bullet}$, exhibiting a complex isotopic pattern due to the presence of both ruthenium and chlorine. The most intensive peak of the pattern at *m/z* 626.12 can be assigned to $[C_{31}H_{38}{}^{35}Cl_2N_2O{}^{102}Ru]^{+\bullet}$, and the second most intensive at *m/z* 628.12 to both $[C_{31}H_{38}{}^{35}Cl{}^{37}ClN_2O{}^{102}Ru]^{+\bullet}$ and $[C_{31}H_{38}{}^{35}Cl_2N_2O{}^{104}Ru]^{+\bullet}$. As can be seen from the insets in Figure 5, the experimental and calculated isotopic patterns are in very good agreement even though the noise level of around 0.4% relative intensity (s/*n* = 250) is not the best. Triplicate spectra are compiled in Supplementary Figure S15.

Comparison with the JEOL Standard FD Source Strictly speaking, a comparison between the new source presented here and JEOL's own AccuTOF FD source would require operating the sources on the same instrument. To get at least an impression of the performance, we compare the LIFDI mass spectra of two ionic liquids (ILs) and of rough pump oil with those published by JEOL in two application notes [61, 62]. The first IL, *N*-butyl-3-methylpyridinium dicyanamide, $[C_{10}H_{16}N]^+$ $[C_2N_3]^-$, shares the cation, $[C]^+$, with the published data, the second IL, 1-butyl-1-methylpyrrolidinium bis(trifluormethylsulfonyl)imide, $[C_9H_{20}N]^+$ $[C_2F_6NO_4S_2]^-$, the anion, $[A]^-$. The LIFDI spectra obtained using our new source both show the respective cation signal at *m/z* 150.12 and *m/z* 142.16 (Figure 6). The spectra measured at an emitter heating rate of 52 mA min^{-1} (same as in Ref. [61]) have noise levels of 0.05% relative intensity (s/*n* = 2000) and 0.015% relative intensity (s/*n* = 6600), respectively. The intensity of the *N*-butyl-3-methylpyridinium cation, $[C_{10}H_{16}N]^+$, *m/z* 150.12, was at 45,000–72,000 counts (triplicate spectra are compiled in Supplementary Figures S16–S17) and are thus equal to what was published in the application note (60,000 counts). The intensity of the 1-butyl-1-methylpyrrolidinium cation, $[C_9H_{20}N]^+$, *m/z* 142.16, even reaches up to 187,000 counts. In addition to the cations, signals corresponding to $[C_2A]^-$ cluster ions appear at *m/z* 355.22 and at *m/z* 564.17, respectively, as is expected for ILs [34, 61].

The LIFDI spectrum of Balzers P3 rough pump oil is also very similar to JEOL's data of a comparable sample [62] and shows a distribution of hydrocarbon molecular ions, most of them in the *m/z* 300–750 range (triplicate spectra are compiled in Supplementary Figure S18). We are thus confident that the LIFDI source presented here provides a performance level comparable with that of JEOL's FD source.

Comparison with LIFDI Using a Magnetic Sector Instrument Finally, selected samples were also analyzed using the FI/FD/LIFDI source and probe installed on the JEOL JMS-700 magnetic sector mass spectrometer (BE) to obtain a comparison of the results with those from a well-established instrument in our lab [31, 32, 34, 35, 37, 63].

The FI-BE mass spectrum of heptane showed the molecular ion, $[C_7H_{14}]^{+\bullet}$, at *m/z* 100.11 and had a signal-to-noise ratio of ca. 4000 (Supplementary Figure S19). In addition, two additional peaks of 0.2% relative intensity were observed at nominal *m/z* 71 and 72 that can be assigned to losses of $C_2H_5^\bullet$ (29 u) and C_2H_4 (28 u) respectively. Upon closer examination of FI-TOF spectra of heptane covering this *m/z* range, peaks at *m/z* 70 (2.5%) and *m/z* 71 (2.0%) were found that can be attributed to losses of C_2H_6 (30 u) and $C_2H_5^\bullet$ (29 u, Supplementary Figure S10). Either of the signals can reasonably be correlated to some degree of fragmentation of the molecular ion; however, the fragments observed using the TOF analyzer are by one hydrogen lower in mass and about ten times more abundant than in the case of the BE instrument.

The LIFDI-BE mass spectrum of dotriacontane exhibited the molecular ion peak at *m/z* 450.54 and the spectrum accumulated during the entire period of desorption/ionization had a signal-to-noise ratio of ca. 3500 (Supplementary Figure S20). Closer examination of this LIFDI spectrum showed the same hydrocarbon impurities at *m/z* 422.51, 436.52, and 464.53 as already noted when describing the TOF spectrum; however,

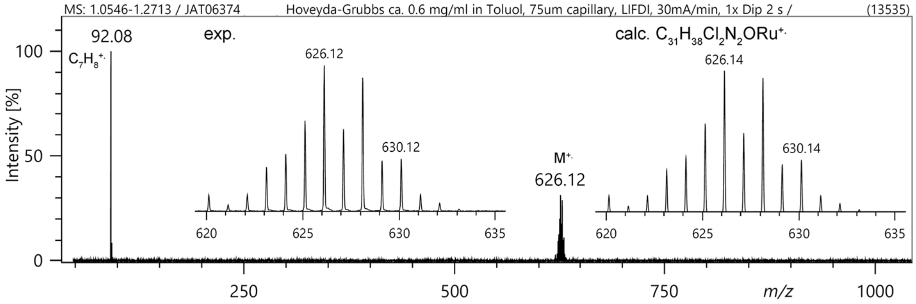

Figure 5. LIFDI spectrum of the Hoveyda–Grubbs II catalyst, $C_{31}H_{38}Cl_2N_2ORu$, dissolved in toluene at 0.6 mg mL^{-1}. The toluene molecular ion, *m/z* 92.08, was present during the run due to toluene continuously flowing through the capillary. The insets show the molecular ion of the catalyst (*left*) to have a complex isotopic pattern that is in very good agreement with the calculated isotopic distribution (*right*)

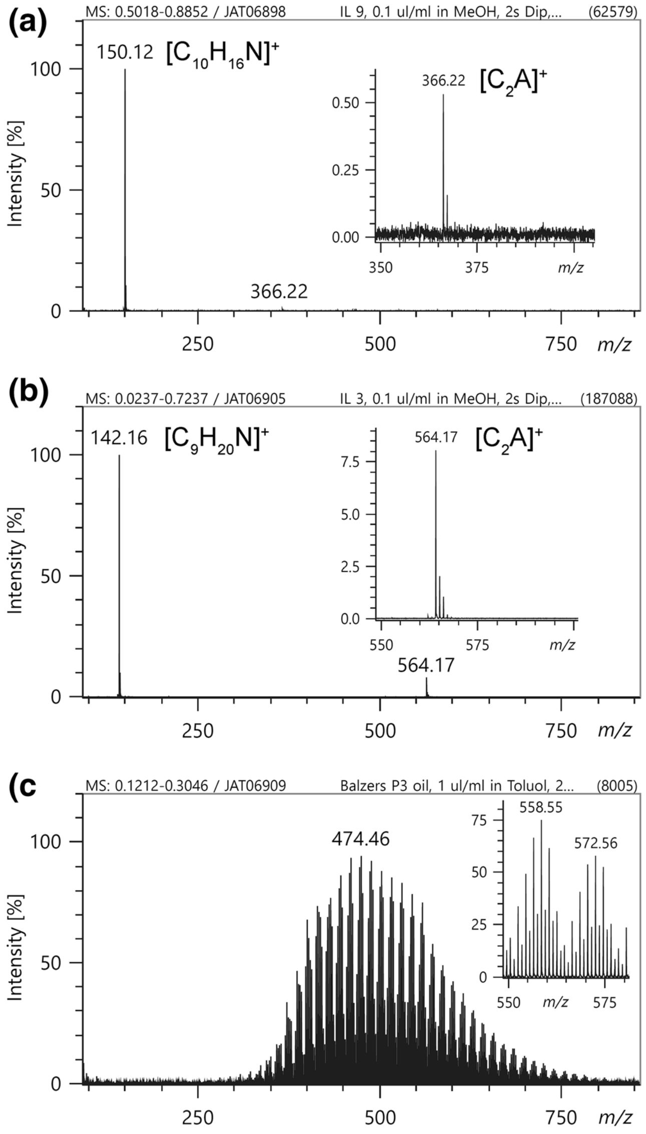

Figure 6. LIFDI mass spectra of (**a**) the ionic liquid *N*-butyl-3-methylpyridinium dicyanamide, $[C_{10}H_{16}N]^+$ $[C_2N_3]^-$; (**b**) the ionic liquid 1-butyl-1-methylpyrrolidinium bis(trifluormethylsulfonyl)imide, $[C_9H_{20}N]^+$ $[C_2F_6NO_4S_2]^-$; and (**c**) of Balzers P3 rough pump oil. The insets of (**a**) and (**b**) show the first cluster ion, $[C_2A]^+$, at *m/z* 366.22 and *m/z* 564.17, respectively. The inset in (**c**) shows an expanded view of the distribution of hydrocarbon molecular ions in the *m/z* 550–580 range. Spectra are averages across the ion production interval. The intensity in counts is displayed at the upper right corner of each plot

the additional low-intensity fragment ion signals caused by radical losses were essentially absent.

The slightly increased fragmentation of molecular ions on the TOF system compared with the BE analyzer may be attributed to either different ion lifetime requirements or to some degree of collision-induced dissociation (CID) in the ion source region. Taking the dotriacontane molecular ion as an example, the overall ion lifetime requirements can be estimated as follows: at 7 keV of kinetic energy, an ion of *m/z* 450 travels at 54,780 m s^{-1}, and thus, it takes the ion 36.5 μs to travel a 2-m path across the BE analyzer. The same ion at 42 eV will travel at 4242 m s^{-1} from the emitter to the orthogonal pulser of the TOF analyzers. Passing along this short path of 0.1 m thus takes 23.6 μs. Also at 7 keV, the passage along the 1.5-m path in the reflector TOF takes 27.4 μs. The overall flight time of 51.0 μs, roughly 1.4 times more than 36.5 μs in the BE instrument, is not significantly longer, and therefore, should not notably increase the degree of ion fragmentation. It may therefore be assumed that some CID has to be taken into account, probably due to slightly increased pressure in close proximity to the emitter. This can be caused by the effluent gas from the GC capillary and by the tighter enclosure of the emitter inside the source compared with the more open construction of the FI/FD/LIFDI source of the BE instrument.

The LIFDI-BE mass spectrum of the Hoveyda–Grubbs II catalyst showed the molecular ion peak at *m/z* 626.18 and had a signal-to-noise ratio of ca. 100 (Supplementary Figure S21). Here, the LIFDI-TOF clearly provides superior data in terms of better s/n (250 vs. 100), higher mass resolution, and higher reproducibility of the isotopic pattern.

To summarize this brief comparison, the results from the new setup on the TOF system were close to those from the BE instrument. Nonetheless, some differences were observed in terms of mass resolution, mass accuracy, signal-to-noise ratio, and fragmentation. While the sector instrument delivered spectra of dotriacontane showing no fragment ion peaks, the AccuTOF caused some degree of alkyl loss. The BE instrument also yielded better signal-to-noise ratio in the case of heptane and dotriacontane while the AccuTOF was notably better in the case of the transition metal complex. In addition, the AccuTOF delivered higher resolving power ($R_{10\%}$ of 6000) than the (aged) BE instrument ($R_{10\%}$ of 1500) as well as superior mass accuracy of ± 0.02 u versus ± 0.06 u. Weighing all the differences, in our opinion, reveals an advantage to the AccuTOF over the BE sector instrument.

Conclusions

We have described a new implementation of an ion source for FI, FD, and LIFDI designed for use on JEOL AccuTOF GC instruments. In contrast to previous designs, the new setup is self-supplied in terms of power supplies, computer control, and emitter observation. Even more important, it allows quick and facile swapping of ion sources within a few minutes without the need to exchange the ion focusing lens stack or to modify the GC transfer line. The field emitter may be heated at up to 60 mA min^{-1} under emission control, which provides high safety of LIFDI operation. In fact, not a single field emitter has been destroyed by discharges since the first trials with the LIFDI source in our lab. We have described the operation of this LIFDI source and probe combination and demonstrated its use by application to typical samples ranging from volatile hydrocarbons over polymers to a water- and moisture-sensitive transition metal catalyst. The spectra obtained were in accordance with those obtained using JEOL's established FD sources for the AccuTOF GC series and the JMS-700 magnetic sector instrument. The setup shall further be explored in terms of high mass and eventually accurate mass capabilities in due course.

Acknowledgements

We are indebted to Dr. Uwe Linne and Jan Bamberger (Philipps-Universität Marburg) for support during the process of development by measuring samples on their AccuTOF for comparison. A gift of polystyrene standards PS 484 and PS 1050 from Dr. Steffen Weidner (Federal Institute for Materials Research and Testing, Berlin) is gratefully acknowledged.

References

1. Müller, E.W.: Feldemission. Ergebn. exakt. Naturw. **27**, 290–360 (1953)
2. Gomer, R., Inghram, M.G.: Applications of field ionization to mass spectrometry. J. Am. Chem. Soc. **77**, 500–500 (1955)
3. Inghram, M.G., Gomer, R.: Mass-spectrometric analysis of ions from the field microscope. J. Chem. Phys. **22**, 1279–1280 (1954)
4. Inghram, M.G., Gomer, R.: Mass-spectrometric investigation of the field emission of positive ions. Z. Naturforsch. A. **10**, 863–872 (1955)
5. Beckey, H.D.: Mass spectrographic investigations, using a field emission ion source. Z. Naturforsch. A. **14**, 712–721 (1959)
6. Beckey, H.D.: Field-ionization mass spectra of organic molecules. Normal C_1 to C_9 paraffins. Z. Naturforsch. A. **17**, 1103–1111 (1962)
7. Beckey, H.D., Wagner, G.: Field ionization mass spectra of organic molecules. II. Amines. Z. Naturforsch. A. **20**, 169–175 (1965)
8. Beckey, H.D.: Analysis of solid organic natural products by field ionization mass spectrometry. Fresenius Z. Anal. Chem. **207**, 99–104 (1965)
9. Beckey, H.D.: Field desorption mass spectrometry: a technique for the study of thermally unstable substances of low volatility. Int. J. Mass Spectrom. Ion Phys. **2**, 500–503 (1969)
10. Beckey, H.D., Heindrichs, A., Winkler, H.U.: New field desorption techniques. Int. J. Mass Spectrom. Ion Phys. **3**, A9–A11 (1970)
11. Beckey, H.D., Hilt, E., Schulten, H.-R.: High temperature activation of emitters for field ionization and field desorption spectrometry. J. Phys. E: Sci. Instrum. **6**, 1043–1044 (1973)
12. Linden, H.B., Hilt, E., Beckey, H.D.: High-rate growth of dendrites on thin wire anodes for field desorption mass spectrometry. J. Phys. E: Sci. Instrum. **11**, 1033–1036 (1978)
13. Linden, H.B., Beckey, H.D., Okuyama, F.: On the mechanism of cathodic growth of tungsten needles by decomposition of hexacarbonyltungsten under high-field conditions. Appl. Phys. **22**, 83–87 (1980)
14. Rabrenovic, M., Ast, T., Kramer, V.: Alternative organic substances for generation of carbon emitters for field desorption mass spectrometry. Int. J. Mass Spectrom. Ion Phys. **37**, 297–307 (1981)
15. Schulten, H.-R., Lehmann, W.D.: High-resolution field desorption mass spectrometry. Part VII. Explosives and explosive mixtures. Anal. Chim. Acta. **93**, 19–31 (1977)
16. Schulten, H.-R.: Recent advances in field desorption mass spectrometry. Adv. Mass Spectrom. **7A**, 83–97 (1978)
17. Giessmann, U., Röllgen, F.W.: Electrodynamic effects in field desorption mass spectrometry. Int. J. Mass Spectrom. Ion Phys. **38**, 267–279 (1981)
18. Wong, S.S., Giessmann, U., Karas, M., Röllgen, F.W.: Field desorption of sucrose studied by combined optical microscopy and mass spectrometry. Int. J. Mass Spectrom. Ion Process. **56**, 139–150 (1984)
19. Davis, S.C., Natoli, V., Neumann, G.M., Derrick, P.J.: A model of ion evaporation tested through field desorption experiments on glucose mixed with alkali metal salts. Int. J. Mass Spectrom. Ion Process. **78**, 17–35 (1987)
20. Beckey, H.D.: Pergamon. Elmsford. (1971)
21. Sammons, M.C., Bursey, M.M., White, C.K.: Field desorption mass spectrometry of onium salts. Anal. Chem. **47**, 1165–1166 (1975)
22. Beckey, H.D., Schulten, H.-R.: Field desorption mass spectrometry. Angew. Chem. Int. Ed. **14**, 403–415 (1975)
23. Beckey, H.D. Pergamon Press, Oxford (1977)
24. Wood, G.W.: Field desorption mass spectrometry: applications. Mass Spectrom. Rev. **1**, 63–102 (1982)
25. Reynolds, W.D.: Field desorption mass spectrometry. Anal. Chem. **51**, 283A–293A (1979)
26. Schulten, H.-R.: Ion formation from organic solids: analytical applications of field desorption mass spectrometry. In: Benninghoven A (ed.). Springer-Verlag, Heidelberg, (1983)
27. Lattimer, R.P., Schulten, H.-R.: Field desorption of hydrocarbon polymers. Int. J. Mass Spectrom. Ion Phys. **52**, 105–116 (1983)
28. Lattimer, R.P., Schulten, H.-R.: Field ionization and field desorption mass spectrometry: past, present, and future. Anal. Chem. **61**, 1201A–1215A (1989)
29. Prókai, L. Marcel Dekker, N. Y. (1990)
30. Evans, W.J., DeCoster, D.M., Greaves, J.: Evaluation of field desorption mass spectrometry for the analysis of polyethylene. J. Am. Soc. Mass Spectrom. **7**, 1070–1074 (1996)
31. Gross, J.H., Weidner, S.M.: Influence of electric field strength and emitter temperature on dehydrogenation and C-C cleavage in field desorption mass spectrometry of polyethylene oligomers. Eur. J. Mass Spectrom. **6**, 11–17 (2000)
32. Gross, J.H., Vékey, K., Dallos, A.: Field desorption mass spectrometry of large multiply branched saturated hydrocarbons. J. Mass Spectrom. **36**, 522–528 (2001)
33. Lattimer, R.P.: Field ionization (FI-MS) and field desorption (FD-MS). In: Montaudo G, Lattimer RP (eds.). CRC Press, Boca Raton, (2001)
34. Gross, J.H.: Liquid injection field desorption/ionization mass spectrometry of ionic liquids. J. Am. Soc. Mass Spectrom. **18**, 2254–2262 (2007)
35. Gross, J.H.: Molecular ions of ionic liquids in the gas phase. J. Am. Soc. Mass Spectrom. **19**, 1347–1352 (2008)
36. Linden, H.B.: Liquid injection field desorption ionization: a new tool for soft ionization of samples including air-sensitive catalysts and non-polar hydrocarbons. Eur. J. Mass Spectrom. **10**, 459–468 (2004)
37. Gross, J.H., Nieth, N., Linden, H.B., Blumbach, U., Richter, F.J., Tauchert, M.E., Tompers, R., Hofmann, P.: Liquid injection field desorption/ionization of reactive transition metal complexes. Anal. Bioanal. Chem. **386**, 52–58 (2006)
38. Monillas, W.H., Yap, G.P.H., Theopold, K.H.: A tale of two isomers: a stable phenyl hydride and a high-spin (S = 3) benzene complex of chromium. Angew. Chem. Int. Ed. **46**, 6692–6694 (2007)
39. Dransfield, T.A., Nazir, R., Perutz, R.N., Whitwood, A.C.: Liquid injection field desorption/ionization of transition metal fluoride complexes. J. Fluor. Chem. **131**, 1213–1217 (2010)
40. Breunig, H.J., Linden, H.B., Moldovan, O.: Liquid injection field desorption ionization mass spectrometry of cyclic metal carbonyl complexes with tetra-antimony ligands. J. Am. Soc. Mass Spectrom. **24**, 164–166 (2013)
41. Molon, M., Dilchert, K., Gemel, C., Seidel, R.W., Schaumann, J., Fischer, R.A.: Clusters [Ma(GaCp*)b(CNR)c] (M = Ni, Pd, Pt): synthesis, structure, and Ga/Zn exchange reactions. Inorg. Chem. **52**, 14275–14283 (2013)
42. Molon, M., Gemel, C., Fischer, R.A.: Organogallium- and organozinc-rich palladium and platinum clusters. Dalton Trans. **43**, 3114–3120 (2014)
43. Freitag, K., Gemel, C., Jerabek, P., Oppel, M.I., Seidel, R.W., Frenking, G., Banh, H., Dilchert, K., Fischer, R.A.: The σ-aromatic clusters [Zn3]+ and [Zn2Cu]: embryonic brass. Angew. Chem. Int. Ed. **54**, 4370–4374 (2015)
44. Rinn, N., Berndt, J.-P., Kreher, A., Hrdina, R., Reinmuth, M., Schreiner, P.R., Dehnen, S.: Peptide-functionalized organotin sulfide clusters. Organometallics. **35**, 3215–3220 (2016)
45. Hornung, J., Wessing, J., Molon, M., Dilchert, K., Gemel, C., Fischer, R.A.: Chemistry of Hume-Rothery inspired organometallics: selective functionalization of [M(ZnCp*)4(ZnCH3)4] (M = Ni, Pd, Pt) with terminal alkynes to yield [M(ZnCp*)4(ZnCCSiiPr)4]. J. Organomet. Chem. **860**, 78–84 (2018)
46. Hoidn, C.M., Leitl, J., Ziegler, C.G.P., Shenderovich, I.G., Wolf, R.: Halide-substituted phosphacyclohexadienyl iron complexes: covalent structures vs. ion pairs. Eur. J. Inorg. Chem. **2019**, 1567–1574 (2019)
47. Heitkemper, T., Sindlinger, C.P.: Electronic push–pull modulation by peripheral substituents in pentaaryl boroles. Chem. Eur. J. **25**, 6628–6637 (2019)

48. Kuehn, L., Jammal, D.G., Lubitz, K., Marder, T.B., Radius, U.: Stoichiometric and catalytic Aryl−Cl activation and borylation using NHC-stabilized nickel(0) complexes. Chem. Eur. J. **0**, (2019)
49. Meier, M., Ji, L., Nitsch, J., Krummenacher, I., Deißenberger, A., Auerhammer, D., Schäfer, M., Marder, T.B., Braunschweig, H.: Preparation and characterization of a π-conjugated donor–acceptor system containing the strongly electron-accepting tetraphenylborolyl unit. Chem. Eur. J. **25**, 4707–4712 (2019)
50. Schaub, T.M., Linden, H.B., Hendrickson, C.L., Marshall, A.G.: Continuous-flow sample introduction for field desorption/ionization mass spectrometry. Rapid Commun. Mass Spectrom. **18**, 1641–1644 (2004)
51. Smith, D.F., Schaub, T.M., Rodgers, R.P., Hendrickson, C.L., Marshall, A.G.: Automated liquid injection field desorption/ionization for Fourier transform ion cyclotron resonance mass spectrometry. Anal. Chem. **80**, 7379–7382 (2008)
52. Briker, Y., Ring, Z., Iacchelli, A., McLean, N., Rahimi, P.M., Fairbridge, C., Malhotra, R., Coggiola, M.A., Young, S.E.: Diesel fuel analysis by GC-FIMS: aromatics, *n*-paraffins, and isoparaffins. Energy Fuel. **15**, 23–37 (2001)
53. Qian, K., Dechert, G.J.: Recent advances in petroleum characterization by GC field ionization time-of-flight high-resolution mass spectrometry. Anal. Chem. **74**, 3977–3983 (2002)
54. Qian, K., Dechert, G.J., Edwards, K.E.: Deducing molecular compositions of petroleum products using GC-field ionization high resolution time of flight mass spectrometry. Int. J. Mass Spectrom. **265**, 230–236 (2007)
55. Matsuo, T., Matsuda, H., Katakuse, I.: Use of field desorption mass spectra of polystyrene and polypropylene glycol as mass references up to mass 10000. Anal. Chem. **51**, 1329–1331 (1979)
56. Linden, H.B., Gross, J.H.: Reduced fragmentation in liquid injection field desorption/ionization-Fourier transform ion cyclotron resonance mass spectrometry by use of helium for the thermalization of molecular ions. Rapid Commun. Mass Spectrom. **26**, 336–344 (2012)
57. Hejazi, L., Ebrahimi, D., Hibbert, D.B., Guilhaus, M.: Compatibility of electron ionization and soft ionization methods in gas chromatography/orthogonal time-of-flight mass spectrometry. Rapid Commun. Mass Spectrom. **23**, 2181–2189 (2009)
58. Röllgen, F.W., Beckey, H.D.: Surface reactions induced by field ionization of organic molecules. Surf. Sci. **23**, 69–87 (1970)
59. Schulten, H.-R., Beckey, H.D.: Criteria for distinguishing between $M^{+\cdot}$ and $[M+H]^+$ ions in field desorption mass spectra. Org. Mass Spectrom. **9**, 1154–1155 (1974)
60. Linden, H.B., Gross, J.H.: A liquid injection field desorption/ionization-electrospray ionization combination source for a Fourier transform ion cyclotron resonance mass spectrometer. J. Am. Soc. Mass Spectrom. **22**, 2137–2144 (2011)
61. Analysis of an ionic liquid by using field desorption (FD) ionization, MS Tips 113, JEOL USA, https://www.jeolusa.com/DesktopModules/Bring2mind/DMX/API/Entries/Download?EntryId=663&Command=Core_Download&language=en-US&PortalId=2&TabId=337,
62. Monitoring rotary vacuum pump oil degradation by using field desorption (FD)-TOFMS and group-type analysis software, MS Tips 98, JEOL USA, https://www.jeolusa.com/DesktopModules/Bring2mind/DMX/API/Entries/Download?EntryId=652&Command=Core_Download&language=en-US&PortalId=2&TabId=337,
63. Siegler, F., Wolff, J.J., Gross, J.H.: Analysis of ferrocenyl compounds by LR and HR field desorption mass spectrometry. Adv. Mass Spectrom. **14**, B083140/083141–B083140/083121 (1998)